

# FREQUENCY RESPONSE OF THE BOUNDARY LAYER ON WALL TRANSFER PROBES

GILEAD FORTUNA and T. J. HANRATTY

Department of Chemical Engineering, University of Illinois, Urbana, Illinois 61801, U.S.A.

(Received 6 November 1970 and in revised form 5 January 1971)

**Abstract**—The time response of the concentration or temperature boundary layer can have a significant effect on measurements of the fluctuating velocity gradient made with wall heat transfer or mass transfer probes. This paper analyzes this effect by carrying out finite difference solutions for a scalar boundary layer under the influence of a harmonic oscillation in the velocity field. The principal assumptions used in the calculations are that the fluctuating scalar field is described by a linearized form of the conservation equation and that the velocity varies linearly with distance from the wall. The frequency response improves with decreasing Schmidt number or Prandtl number.

## NOMENCLATURE

A, correction factor for the pseudo steady state solution, defined by equation (26);  
 B, coefficient of  $f_2$  profile, equation (19);  
 D, diameter of circular transfer element;  
 F, temperature or concentration;  
 $F_b$ , bulk temperature or bulk concentration;  
 $\bar{F}$ , average of F;  
 $f$ , fluctuating component of F, equation (4);  
 $\hat{f}$ , amplitude of  $f$  fluctuation;  
 $f_1$ , dimensionless  $\hat{f} = f(\bar{s}/\delta)$ ;  
 $f_{1R}$ , real part of  $f_1$ ;  
 $f_{1I}$ , imaginary part of  $f_1$ ;  
 $f_s$ , pseudo steady state approximation for  $f_1$ ;  
 $f_2$ ,  $= f_1 - f_s/i\omega^*$ ;  
 K, mass transfer coefficient for the probe;  
 $\bar{K}$ , average value of K;  
 $k$ , fluctuating component of K;  
 $\bar{k}^2$ , average value of  $k^2$ ;  
 L, length of transfer element;  
 $L^+$ , normalized length of the transfer element  $= L(u^*/v)$ ;  
 n, frequency in cycles per s;  
 N, Schmidt number or Prandtl number;  
 S, velocity gradient at the wall;  
 $\bar{S}$ , average velocity gradient at the wall;  
 s, fluctuating component of S, equation (3);

$\bar{s}^2$ , average value of  $s^2$ ;  
 t, time;  
 U, axial velocity;  
 $u^*$ , friction velocity;  
 $W_s$ , spectral density function for  $\bar{s}^2$ ;  
 $W_k$ , spectral density function for  $\bar{k}^2$ ;  
 x, distance in flow direction along the transfer element;  
 $x^+$ ,  $= x(u^*/v)$ ;  
 y, distance perpendicular to the wall;  
 $y^+$ ,  $= y(u^*/v)$ ;  
 $y^*$ ,  $= y^+ N^{\frac{1}{2}}$ ;  
 $\alpha$ , diffusivity for mass or heat;  
 $\beta$ , parameter appearing in equation (12);  
 $\delta_{cs}$ , scalar boundary layer thickness;  
 $\delta_c^+$ ,  $= \delta_c(u^*/v)$ ;  
 $\theta$ ,  $=$  phase lag of  $(\partial f^*/\partial y^*)_{y^*=0}$  with  $s$ ;  
 $\nu$ ,  $=$  kinematic viscosity;  
 $\omega$ ,  $= 2\pi n$ ;  
 $\omega^*$ ,  $= \omega(u^{*2}/v) N^{\frac{1}{2}}$ .

## 1. INTRODUCTION

WALL MASS transfer probes and heat transfer probes [6–8] have been used in a number of recent investigations to study the fluctuations in the velocity gradient at a wall. One of the chief difficulties in interpreting these measurements has been the need to correct for the frequency

response of the concentration or temperature boundary layer. This paper presents a solution to this problem.

The principal assumptions used in the analysis are that the fluctuating scalar field is described by a linearized form of the conservation equation and that the velocity varies linearly with distance from the wall throughout the scalar boundary layer. The solution that is presented is obtained by finite difference approximations. This approach had been used by Mitchell and Hanratty [3]. However, instabilities in their numerical techniques limited the range of applicability of their results to low frequencies. We have been able to overcome the difficulties experienced by Mitchell and Hanratty and therefore, can present results for the entire frequency range. The numerical integration agrees with the asymptotic solutions outlined by Lighthill [9] and by Bellhouse and Schultz [7] for high frequencies and for low frequencies. The general mathematical approach is similar to that used by Fagella-Alabastro and Hellums [10] in their study on diffusion in pulsating flow.

2. DEFINING EQUATIONS

Consider a rectangular transfer element embedded flush with a solid wall with its long side perpendicular to the direction of mean flow. In this configuration the rate of transfer will not be sensitive to velocity fluctuations in the transverse direction [11]. The length of the element is designated by  $L$  and the width is large enough that diffusion in the transverse direction can be neglected. We consider situations such that

$$\frac{u^{*2}L^2}{\nu\alpha} < 5000$$

so that diffusion in the direction of mean flow can also be neglected [12]. The thickness of the scalar boundary layer is assumed to be thin enough that velocities normal to the surface can be neglected and the velocity field is given as

$$U = Sy \tag{1}$$

where  $S$  is the velocity gradient at the wall.

If we let  $F$  designate either a temperature or a concentration, the conservation equation is

$$\frac{\partial F}{\partial t} + Sy \frac{\partial F}{\partial x} = \alpha \frac{\partial^2 F}{\partial y^2}. \tag{2}$$

Here  $x$  is the direction of mean flow,  $y$  the distance perpendicular to the wall and  $\alpha$  the diffusivity. Equation (2) is to be solved using boundary conditions

$$\begin{aligned} F(x, 0, t) &= 0 & 0 \leq x \leq L \\ F(x, \infty, t) &= F(0, y, t) = F_b. \end{aligned} \tag{3}$$

Define  $F$  and  $S$  as the sum of a time averaged term and a fluctuating term.

$$\begin{aligned} F &= \bar{F} + f \\ S &= \bar{S} + s. \end{aligned} \tag{4}$$

We obtain equations for  $\bar{F}$  and  $f$  by substituting (4) into (2) and neglecting second order terms in the fluctuating components.

$$\bar{S}y \frac{\partial \bar{F}}{\partial x} = \alpha \frac{\partial^2 \bar{F}}{\partial y^2} \tag{5}$$

$$\frac{\partial f}{\partial t} + \bar{S}y \frac{\partial f}{\partial x} + sy \frac{\partial \bar{F}}{\partial x} = \alpha \frac{\partial^2 f}{\partial y^2}. \tag{6}$$

The boundary conditions for (5) and (6) are

$$\begin{aligned} \bar{F}(x, 0) &= f(x, 0, t) = 0 & 0 \leq x \leq L \\ \bar{F}(x, \infty) &= \bar{F}(0, y) = F_b \\ f(x, \infty, t) &= f(0, y, t) = 0. \end{aligned} \tag{7}$$

The solution to (5) is given by Reiss [2] as

$$\frac{\bar{F}}{F_b} = \frac{1}{\Gamma(\frac{3}{2})} \int_0^\eta e^{-z^2} dz \tag{8}$$

where

$$\eta = y \left( \frac{\bar{S}}{9\alpha x} \right)^{\frac{1}{2}} = y^+ N^{\frac{1}{2}} \left( \frac{1}{9x^+} \right)^{\frac{1}{2}}$$

and  $N$  is the Schmidt number or Prandtl number,  $y^+$  and  $x^+$  distances made dimensionless with respect to wall parameters  $u^*$  and  $\nu$ .

We seek a solution for the fluctuating scalar field for a harmonic variation of  $s$

$$s = \hat{s}e^{i\omega t} \tag{9}$$

where  $\delta$  and  $\omega$  are real numbers. Since the equation for  $f$  is linear,

$$f = \hat{f}e^{i\omega t} \tag{10}$$

where  $\hat{f}$  can be a complex number. The following equation is obtained for

$$f_1 = \hat{f} \frac{\delta}{\delta}$$

by substituting (9) and (10) into (6).

$$i\omega^* f_1 + y^* \frac{\partial f_1}{\partial x^+} + y^* \frac{\partial \bar{F}}{\partial x^+} = \frac{\partial^2 f_1}{\partial y^{*2}} \tag{11}$$

where

$$y^* = y^+ N^{\frac{1}{2}}$$

and

$$\omega^* = \frac{\omega v}{u^{*2}} N^{\frac{1}{2}}$$

### 3. HIGH FREQUENCY AND LOW FREQUENCY SOLUTIONS

Lighthill [9] has argued that the term

$$y^* \frac{\partial f_1}{\partial x^+}$$

can be neglected at high frequencies ( $\omega^* \delta_c^+$ , a large number). Using this simplification (11) can be integrated to give

$$\begin{aligned} f_1 &= \frac{2\beta}{\omega^* x^{+\frac{3}{2}}} \exp[-\sqrt{(i\omega^*)} y^*] \\ &- \frac{2\beta}{\omega^{*2} x^{+\frac{3}{2}}} \exp(-\eta^3) \\ &+ \frac{\beta y^{*2}}{i\omega^* x^{+\frac{3}{2}}} \exp(-\eta^3) \end{aligned} \tag{12}$$

and

$$\frac{\partial f_1}{\partial y^*} = -\frac{2\beta}{x^{+\frac{3}{2}} \omega^{*\frac{3}{2}}} \sqrt{i} \tag{13}$$

where

$$\beta = \frac{F_b}{(3)(9)^{\frac{1}{2}} \Gamma^{\frac{3}{2}}}$$

Again, following the analysis outlined by Lighthill [9] a low frequency solution ( $\omega^* \delta_c^+$ , a small number) can be obtained by using the following approximation

$$f_1 = f_s + i\omega^* f_2 \tag{14}$$

where we call  $f_s$  the pseudo-steady state approximation. The following equation for  $f_s$  and  $f_2$  are obtained by substituting (14) into (11) and assuming that  $\omega^*$  is a small number

$$y^* \frac{\partial f_s}{\partial x^+} + y^* \frac{\partial \bar{F}}{\partial x^+} = \frac{\partial^2 f_s}{\partial y^{*2}} \tag{15}$$

$$f_s + y^* \frac{\partial f_2}{\partial x^+} = \frac{\partial^2 f_2}{\partial y^{*2}} \tag{16}$$

Equations (15) and (16) are to be solved for the conditions of  $f_s$  and  $f_2$  being zero at the wall and at large distances from the wall. The solution to (15) is

$$f_s = s \frac{\partial \bar{F}}{\partial \bar{S}} = \frac{1}{3} y^* \frac{\partial \bar{F}}{\partial y^*} \tag{17}$$

We seek an approximate solution to (16) by using the integral form of the conservation equation

$$\left( \frac{\partial f_2}{\partial y^*} \right)_{y^*=0} = \frac{d}{dx} \int_0^\infty y^* f_2 dy^* + \int_0^\infty f_s dy^* \tag{18}$$

The following relation satisfies the conditions that  $f_2$  and its second derivative are zero at the wall and that  $f_2$  and its first and second derivatives are zero at large distances from the wall

$$f_2 = Bx^{+\frac{3}{2}} y^* \frac{\partial \bar{F}}{\partial y^*} \tag{19}$$

By substituting (19) and (8) into (18) we calculate that

$$B = 0.210. \tag{20}$$

We therefore obtain the following relation for low frequencies

$$\left(\frac{\partial f_1}{\partial y^*}\right)_{y^*=0} = \frac{\beta}{x^{+\frac{1}{2}}} - i\omega^* (0.610) \beta x^{+\frac{1}{2}}. \quad (21)$$

4. NUMERICAL RESULTS

The numerical solution for (11) was obtained by using the Crank–Nicholson six point implicit method [13]. The mesh sizes in both the  $x^+$  and  $y^*$  directions were varied in order to check the accuracy of the calculations.

Values of

$$\left(\frac{\partial f_1}{\partial y^*}\right)_{y^*=0}$$

were determined as a function of  $x^+$  for different  $\omega^*$ . These agree with the asymptotic solutions outlined in the previous section for high and low frequencies. Figures 1 and 2 give a comparison for  $x^+ = 2.54$  of the amplitude of the sinusoidal variation of

$$\left(\frac{\partial f_1}{\partial y^*}\right)_{y^*=0}$$

and of its lag with  $s$ .

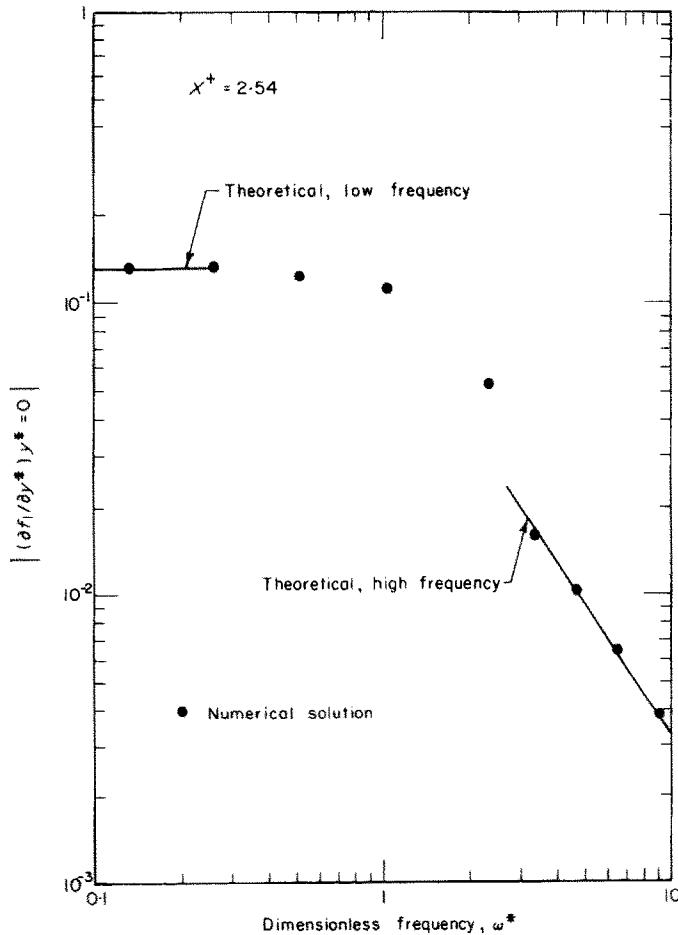


FIG. 1. Amplitude of the sinusoidal variation of the fluctuating velocity gradient.

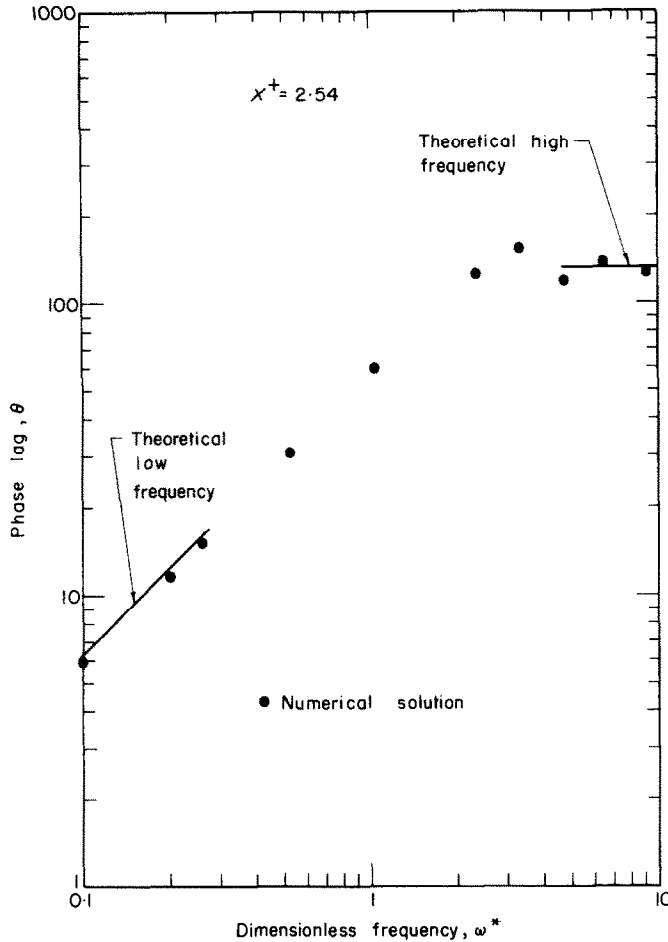


FIG. 2. Phase lag of concentration gradient  $(\partial f_1 / \partial y^*)_{y^* = 0}$  with velocity gradient  $s$ .

The transfer coefficient describing the rate of transfer to the surface of the probe,  $K$ , is given as

$$K = \frac{\alpha}{F_b} \int_0^1 \left( \frac{\partial F}{\partial y} \right)_{y=0} d \left( \frac{x}{L} \right) \quad (22)$$

This can be defined as the sum of a time averaged and a fluctuating component,  $K = \bar{K} + k$ , where

$$\bar{K} = \frac{3}{2\Gamma(\frac{4}{3})9^{\frac{1}{3}}} \left( \frac{\alpha^2 \bar{S}}{L} \right)^{\frac{1}{3}} \quad (23)$$

If a pseudo-steady state solution is used to describe the fluctuating concentration field, the instantaneous value of  $k$  is related to the instantaneous value of  $s$  through the equation

$$\frac{k}{\bar{K}} = \frac{1}{3} \frac{s}{\bar{S}} \quad (24)$$

and the mean-squared value of  $k$  is given as

$$\frac{\bar{k}^2}{\bar{K}^2} = \frac{1}{9} \frac{\bar{s}^2}{\bar{S}^2} \quad (25)$$

We follow the formulation of Mitchell and Hanratty [3] in using the results of the numerical integration of (11). Since the fluctuating concentration field is related to the fluctuating velocity gradient at the wall through a linear equation, the spectral density function for  $\bar{s}^2$ ,  $W_s$ , can be

$$A = \frac{\int_0^{L^+} \left| \frac{\partial f_1}{\partial y^*} \right|_{y^*=0} dx^+}{\int_0^{L^+} \left| \frac{\partial f_s}{\partial y^*} \right|_{y^*=0} dx^+} \quad (27)$$

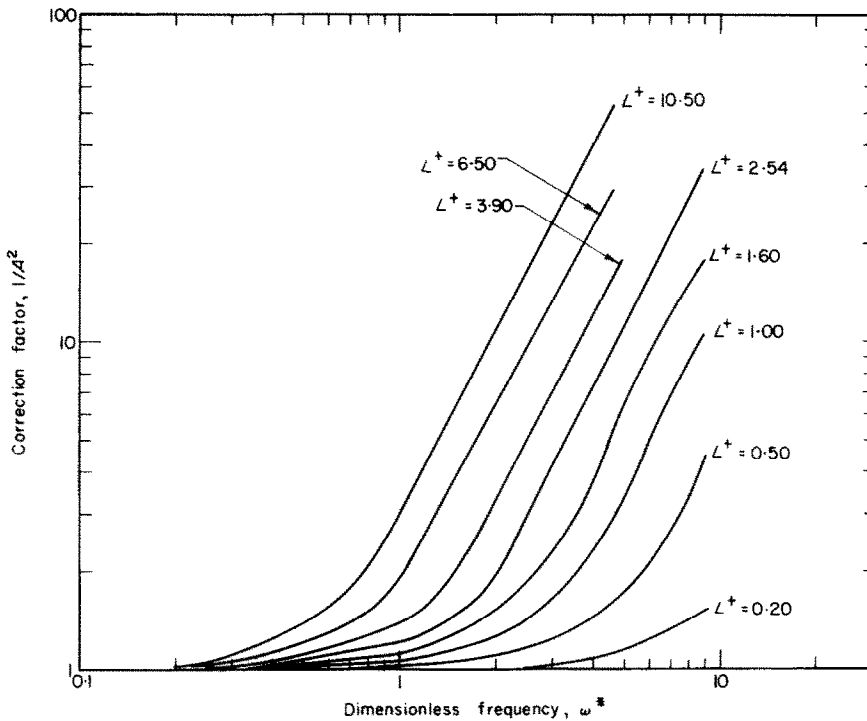


FIG. 3. Correction factor for pseudo-steady state solution.

related to the spectral density function for  $\bar{k}^2$ ,  $W_k$ , where by the equation

$$W_s = 9 \frac{\bar{S}^2}{\bar{K}^2} \frac{W_k}{A^2} \quad (26)$$

where the factor  $A^2$  is a function of frequency. It may be regarded as a correction to the pseudo-steady state solution and is therefore equal to unity at low frequencies. The factor  $A$  is related to the numerical solution for  $f_1$  in the following way

$$\left| \frac{\partial f_1}{\partial y^*} \right|^2 = \left( \frac{\partial f_{1R}}{\partial y^*} \right)^2 + \left( \frac{\partial f_{1I}}{\partial y^*} \right)^2 \quad (28)$$

and

$f_{1R}$  = real part of  $f_1$

$f_{1I}$  = imaginary part of  $f_1$ .

Calculated values of  $1/A^2$  are shown in Fig. 3 as functions of  $L^+$  and  $\omega^*$ . It is found that the result reported by Mitchell and Hanratty [3]

$$|A|^2 = \frac{1}{1 + 0.060(L^+)^\frac{5}{3}\omega^{*2}} \quad (29)$$

is correct only if  $L^+ \omega^{*2} \leq 5$ .

The application of these results to determine  $W_s$  from a wall mass transfer probe is illustrated in Fig. 4. The data were obtained for a Reynolds number of 24 500 with a 1 in. pipe [5]. The probe was of circular shape of diameter  $D = 0.004$  in. and the diffusivity and kinematic viscosity characterizing the system are  $\alpha = 8.4 \times 10^{-6}$  cm<sup>2</sup>/s and  $\nu = 0.89 \times 10^{-2}$  cm<sup>2</sup>/s. The measured spectral density function of the mass transfer

fluctuations is plotted as  $9 W_k / \bar{K}^2$ . This would correspond to the pseudo-steady state approximation for  $W_s / S^2$ . The dashed line in Fig. 4 is the calculated curve for  $W_s / S^2$  after the frequency response of the scalar boundary layer has been taken into account using Fig. 3. The scaled turbulence intensity ( $\bar{s}^2 / S^2$ ), which is the area under the curve after correction, is

$$\sqrt{\frac{\bar{s}^2}{S^2}} = 0.349. \quad (30)$$

The pseudo-steady state result, equation (24), yields a turbulence intensity of 0.302, which is

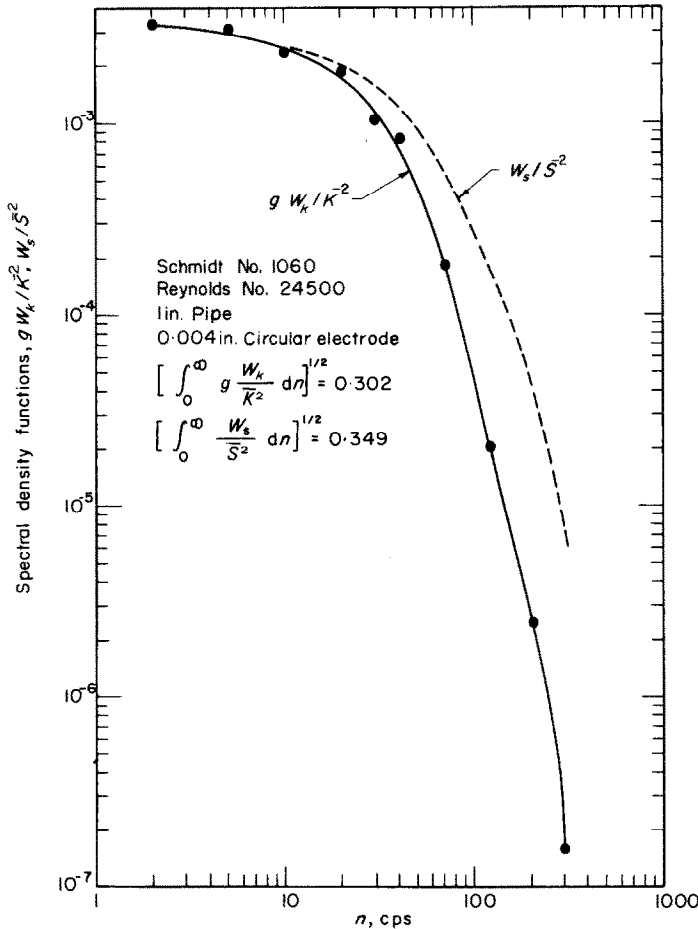


FIG. 4. Spectral density of fluctuation.

the area under the uncorrected curve. The correction for the circular electrode was obtained by integrating the corrected signal over all the electrode surface, thus taking into account the variation of the length,  $L$ , in the direction of flow. This correction is shown in detail in [5]. It is not much different from assuming a rectangular electrode with an effective length of  $0.82 D$  [2].

### 5. COMPARISON OF MASS TRANSFER PROBES AND HEAT TRANSFER PROBES

It is of interest to compare the frequency response of a thermal wall probe with a mass transfer probe in an aqueous system. Mass transfer probes have involved systems with large Schmidt numbers, 1000–3000. For water a thermal probe would be characterized with a Prandtl number of about 5. From Fig. 3 we see that the range of frequencies over which corrections have to be made depends on the Schmidt number or Prandtl number. For example, if we used a probe with an  $L^+ = 1.6$  a 10 per cent correction would have to be made when  $\omega^* = 0.9$ . Since  $\omega^*$  varies directly with the one third power of the Schmidt number or the Prandtl number, the frequency at which this correction need be made is  $(2000/5)^{\frac{1}{3}}$  times greater for the thermal probe than for the mass transfer probe. We conclude that in general thermal probes have a better frequency response than mass transfer probes. This arises because probes with smaller Schmidt numbers or Prandtl numbers have thicker scalar boundary layers and therefore see large convective velocities.

However this increase in the boundary layer thickness sometimes places severe restrictions on the size of the probe required so that the approximation of the velocity field by a linear relation is valid. Define a thickness of the scalar boundary layer  $\delta_c$  as the distance from the wall where  $\bar{F}_b$ . From (8) it follows that

$$\delta_c^+ \cong 2.92 \frac{x^{+\frac{1}{3}}}{N^{\frac{1}{3}}}. \quad (31)$$

If the probe is to be used to measure turbulent velocities close to a wall, it is desirable that  $\delta_c^+ > 1$ . For a mass transfer probe with  $N = 2000$  this is satisfied even for very long probes. However, for a thermal probe with  $N = 5$ , it would be necessary to use probes with  $L^+ \leq 0.20$ .

### ACKNOWLEDGEMENT

This work is being supported by the National Science Foundation under Grant NSF GK 2813X.

### REFERENCES

1. T. J. HANRATTY, Study of turbulence close to a wall, *Physics Fluids Suppl.* S126–S133 (1967).
2. L. P. REISS and T. J. HANRATTY, An experimental study of the unsteady nature of the viscous sublayer, *A.I.Ch.E. JI* **9**, 154 (1963).
3. J. E. MITCHELL and T. J. HANRATTY, A study of turbulence at a wall using an electrochemical wall shear-stress meter, *J. Fluid Mech.* **26**, 199 (1966).
4. K. K. SIRKAR and T. J. HANRATTY, Limiting behaviour of the transverse turbulent velocity fluctuations close to a wall, *I/EC Fundamentals* **8**, (1969).
5. G. FORTUNA, Effect of drag reducing polymers in flow near a wall, Ph.D. Thesis, University of Illinois, Urbana (1970).
6. B. J. BELLHOUSE and D. L. SCHULTZ, The determination of fluctuating velocity in air with heated thin film gauges, *J. Fluid Mech.* **29**, 289 (1967).
7. B. J. BELLHOUSE and D. L. SCHULTZ, The measurement of fluctuating skin friction in air with heated thin-film gauges, *J. Fluid Mech.* **32**, 675 (1968).
8. M. MIYA, Properties of roll waves, Ph.D. Thesis, University of Illinois, Urbana (1970).
9. M. J. LIGHTHILL, The response of laminar skin friction and heat transfer to fluctuations in the steam velocity, *Proc. R. Soc.* **224A**, 1 (1954).
10. E. B. FAGELLA-ALABASTRO and J. D. HELLUMS, A theoretical study on diffusion in pulsating flow, *A.I.Ch.E. JI* **15**, 164 (1969).
11. J. E. MITCHELL, Investigation of wall turbulence using a diffusion-controlled electrode, Ph.D. Thesis, University of Illinois, Urbana (1965).
12. S. C. LING, Heat transfer from a small isothermal spanwise strip on an insulated boundary, *J. Heat Transfer* **85C**, 230 (1963).
13. L. LAPIDUS, *Digital Computation for Chemical Engineers*. McGraw-Hill, New York (1962).



RÉPONSE EN FRÉQUENCE DE LA COUCHE LIMITE THERMIQUE SUR LES PAROIS DE  
SONDES

**Résumé**— La réponse dans le temps de couche limite de concentration ou de température peut avoir un effet significatif sur des mesures de gradient fluctuant de vitesse à l'aide du transfert de chaleur ou de masse sur des sondes. Cet article analyse cet effet en dégageant les solutions aux différences finies pour une couche limite sous l'influence d'une oscillation harmonique du champ des vitesses. Les hypothèses principales formulées sont que le champ scalaire fluctuant est décrit par une forme linéarisée de l'équation de conservation et que la vitesse varie linéairement avec la distance à la paroi. La réponse en fréquence s'améliore quand le nombre de Prandtl ou de Schmidt diminue.

FREQUENZREAKTION DER GRENZSCHICHT AUF SONDEN FÜR  
ÜBERGANGSMESSUNGEN

**Zusammenfassung**—Die Zeitabhängigkeit von Temperatur-oder Konzentrationsgrenzschichten kann einen besonderen Einfluss auf Messungen des Fluktuationsgeschwindigkeitsgradienten haben, bei Verwendung von Messsonden für die Wand-Wärmeübertragung oder Stoffübertragung. In der vorliegenden Arbeit wird dieser Effekt mit einem endlichen Differenzenverfahren für eine skalare Grenzschicht unter der Einwirkung harmonischer Schwingungen auf das Geschwindigkeitsfeld untersucht. Bei der Untersuchung wurde die grundlegende Annahme getroffen, dass das Fluktuations-Skalar-Feld durch eine linearisierte Form der Kontinuitätsgleichung beschrieben werden kann und dass sich die Geschwindigkeit linear mit dem Wandabstand ändert. Die Frequenz-Reaktion verfeinert sich mit abnehmender Schmidt- bzw. Prandtl-Zahl.

ЧАСТОТНАЯ ХАРАКТЕРИСТИКА ПОГРАНИЧНОГО СЛОЯ НА  
СТЕНКЕ ДАТЧИКОВ ТЕПЛО-И МАССОПЕРЕНОСА

**Аннотация**—Постоянная времени концентрационного или температурного пограничного слоя может оказывать значительное влияние на измерения пульсаций градиента скорости на стенке датчиков тепло-или массопереноса. В данной статье этот эффект анализируется путём проведения решений в конечных разностях для скалярного пограничного слоя с наложением гармонического колебания скоростного поля. При расчёте делались принципиальные допущения, заключающиеся в том, что пульсирующее скалярное поле описывается линеаризованным уравнением сохранения, а скорость изменяется линейно с расстоянием от стенки. Частотная характеристика улучшается с уменьшением числа Шмидта или числа Прандтля.